

## Research Article

# Sufficient Condition for Estimation in Designing $H_{\infty}$ Filter-Based SLAM

Nur Aqilah Othman,<sup>1</sup> Hamzah Ahmad,<sup>1</sup> and Toru Namerikawa<sup>2</sup>

<sup>1</sup>Faculty of Electrical and Electronics Engineering, Universiti Malaysia Pahang, Pekan Campus, 26600 Pekan, Pahang, Malaysia

<sup>2</sup>Department of System Design Engineering, School of Integrated Design Engineering, Keio University, 3-14-1 Hiyoshi, Kohoku-ku, Yokohama 223-8522, Japan

Correspondence should be addressed to Nur Aqilah Othman; [aqilah@ump.edu.my](mailto:aqilah@ump.edu.my)

Received 29 April 2014; Accepted 29 July 2014

Academic Editor: Tofiqh Allahviranloo

Copyright © 2015 Nur Aqilah Othman et al. This is an open access article distributed under the Creative Commons Attribution License, which permits unrestricted use, distribution, and reproduction in any medium, provided the original work is properly cited.

Extended Kalman filter (EKF) is often employed in determining the position of mobile robot and landmarks in simultaneous localization and mapping (SLAM). Nonetheless, there are some disadvantages of using EKF, namely, the requirement of Gaussian distribution for the state and noises, as well as the fact that it requires the smallest possible initial state covariance. This has led researchers to find alternative ways to mitigate the aforementioned shortcomings. Therefore, this study is conducted to propose an alternative technique by implementing  $H_{\infty}$  filter in SLAM instead of EKF. In implementing  $H_{\infty}$  filter in SLAM, the parameters of the filter especially  $\gamma$  need to be properly defined to prevent finite escape time problem. Hence, this study proposes a sufficient condition for the estimation purposes. Two distinct cases of initial state covariance are analysed considering an indoor environment to ensure the best solution for SLAM problem exists along with considerations of process and measurement noises statistical behaviour. If the prescribed conditions are not satisfied, then the estimation would exhibit unbounded uncertainties and consequently results in erroneous inference about the robot and landmarks estimation. The simulation results have shown the reliability and consistency as suggested by the theoretical analysis and our previous findings.

## 1. Introduction

The existence of uncertainties in various forms has caused numerous applications to function not as intended. Until today, their existence is almost inevitable; nonetheless, some devices have been proposed to mitigate such a problem. Although a number of the devices were proven to have succeeded in filtering the noise, the solution still demands further improvements. Owing to the existence of this problem, a robotics application known as simultaneous localization and mapping (SLAM) has experienced difficulties in increasing the efficiency of its estimation. SLAM provides a condition where a mobile robot is assigned to observe an unknown environment and incrementally constructs a map showing the environment that it has recognized. The mobile robot then attempts to localize itself on the constructed map recursively until its task is achieved. SLAM has been applied

in a wide range of applications such as mining, underwater, and space exploration [1–5] through various techniques, for example, 3D visualization [5, 6], multiple robot navigation [7–9], vision-based strategies [10, 11], learning strategies through artificial intelligence [9, 12, 13], and intermittent observation issues [14–16]. Figure 1 depicts a simple notion of SLAM.

A considerable approach that currently seems to be able to tolerate uncertainties in SLAM relies on probabilistic technique. This technique which is based on Bayesian approach is more preferred as compared to the behaviour-based SLAM and mathematical-based SLAM owing to their complexity as well as high computational cost [4]. The probability-based approach takes into account these limitations reasonably well as it does not require extensive mathematical computation nor the demand of high reliability sensors for the position estimation. The extended Kalman filter (EKF) is an example

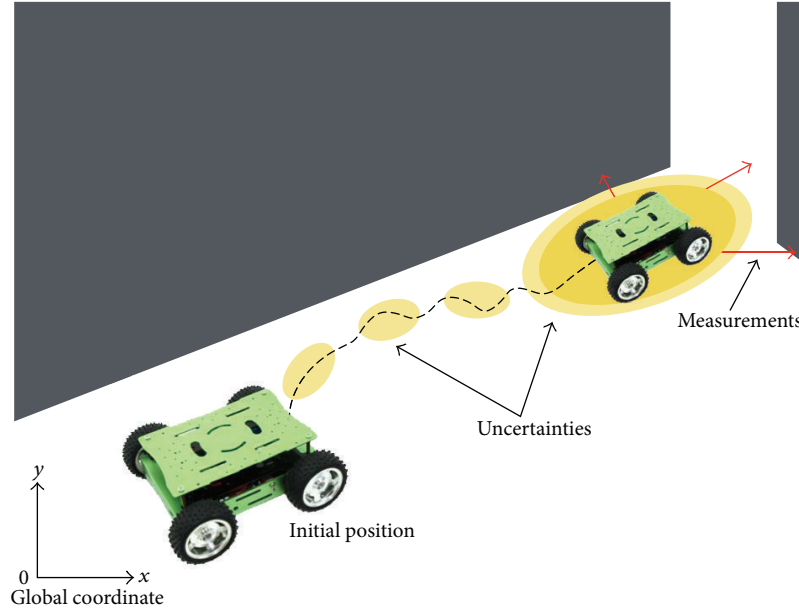


FIGURE 1: Simultaneous localization and mapping: mobile robot makes relative measurements with some uncertainties.

of one of the many probabilistic techniques available. EKF's application in SLAM gained popularity since the early 2000s and still receives high attention among researchers [17–22]. Early development of EKF-based SLAM was proposed by Gamin Disanayake et al. [17, 19] notably due to its ease of application as well as lower computational cost as compared to other probabilistic approaches. Unfortunately, SLAM demands further considerations for the environmental conditions. An assumption of Gaussian noise has restricted EKF performance as the main player thus allowing space for a more robust approach such as the particle filter (PF) [23, 24]. Nonetheless, PF has its drawbacks owing to its complexity as well as higher computational cost. Therefore, in this circumstance,  $H_\infty$  filter approach for SLAM is proposed to mitigate the aforementioned issues as this particular technique is more robust as compared to the EKF as far as the non-Gaussian noise is concerned and it has a much lower computational cost as compared to the PF. A brief description of the filter is discussed in [25].

In this paper,  $H_\infty$  filter-based SLAM performance is further analysed to aid previous work conducted by [2, 26–28]. One of the earliest applications of this technique was reported by [2]. It has been proven that the  $H_\infty$  filter is an alternative solution for SLAM problem in an underwater application. The filter performance has been compared to PF and EKF to identify the performance between each technique. Even though PF has shown better results on the estimation,  $H_\infty$  filter is suggested to be the best solution especially when computational cost and non-Gaussian noise environments are taken into consideration. Further investigations were made on the filter convergence properties as reported by [26, 27, 29].

Despite what  $H_\infty$  filter could offer to SLAM, unlike EKF,  $H_\infty$  filter solution can unboundedly increase and exhibit finite escape time problem as reported by [26, 30].

Therefore, in order to apply  $H_\infty$  filter efficiently to SLAM, the designer must carefully design the filter parameters to achieve the desired and expected performance. Hence, further inspection regarding the filter characteristics has been proposed. Bolzern and Maroni [31] discovered that  $H_\infty$  filter must also satisfy  $P_0 = R^{-1}$  to achieve better estimation. A study for both filtering and prediction stages has been proposed and it was found that, under feasibility and sufficient conditions, the filter is able to achieve a stable result. Furthermore, [27] proposed the covariance inflation [32, 33] and  $\gamma$ -switching strategy as an additional technique to prevent the occurrence of finite escape time. Experimental results supported their analysis and demonstrated that the methods may alternatively avoid finite escape time.

Motivated by the preceding works, further analyses of the  $H_\infty$  filter-based SLAM are proposed to gain more insight into the sufficient conditions for estimation purposes. Based on the preliminary results obtained through theoretical analysis and simulations, it suggests that if some conditions are satisfied, the  $H_\infty$  filter provides a better estimation while at the same time refraining the existence of finite escape time in the estimation. The results obtained are also in good agreement with the previous results. Nevertheless, it is noteworthy to mention that there is also some trade-off between  $\gamma$  and the design parameters especially between the initial state covariance, process, and measurement noises distributions. Besides, as there are many types of environment available, two conditions of different initial state covariance are examined to understand its effect on SLAM with consideration for the process and measurement noises distributions. The analyses are shown to provide the filter characteristics in different situations of environmental conditions.

This paper is organized as follows. Section 2 describes the problem formulation about  $H_\infty$  filter-based SLAM, followed by Section 3 which examines the convergence of  $H_\infty$  filter

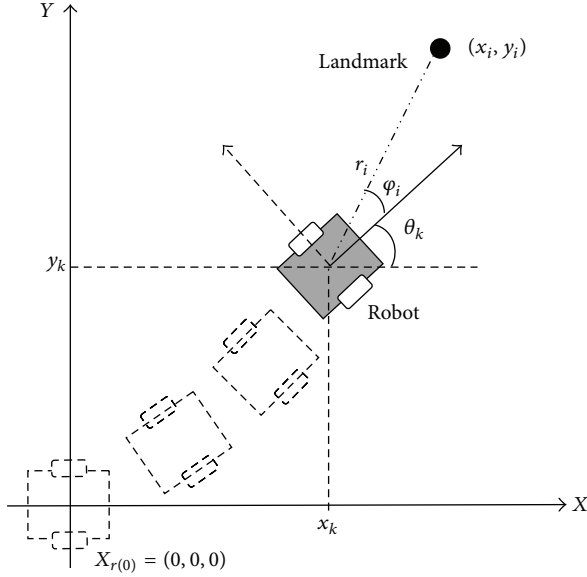


FIGURE 2: Process and measurement model of SLAM.

for SLAM under some conditions. Next, some simulation results which consist of two cases of environmental conditions are demonstrated to evaluate our proposal in Section 4. Finally, Section 5 concludes this paper.

## 2. Problem Statement

The  $H_\infty$  filter-based SLAM is introduced and the model used throughout the study is explained in this section. The state is formulated as a joint state vector of the robot position and the location of the landmarks observed in the environment. The state vector  $X_k \in \mathbb{R}^{3+2m}$  at time  $k$  is represented as

$$X_k = \begin{bmatrix} X_r \\ X_m \end{bmatrix}, \quad (1)$$

where  $X_r = [\theta_k \ x_k \ y_k]^T$  is the position of the mobile robot that is represented by robot heading angle  $\theta_k$  and coordinates of the centre of the mobile robot with respect to the global coordinate frame  $(x_k, y_k)$ . While  $X_m \in \mathbb{R}^{2m}$ ,  $m = 1, 2, \dots, N$  is the location of each respective landmark of  $x_i, y_i$  ( $i = 1, 2, \dots, l$ ) that exist in the environment. The landmarks are modelled as point landmarks.

**2.1. Mobile Robot SLAM Model.** Basically, there are two general steps in providing the system behaviour during mobile robot observations, that is, process and measurement models. Both models are vital to provide necessary information about the surroundings. Moreover, these two models actually ensemble important knowledge about the robot motions and relative information between robot and landmarks which are iteratively updated. A nonlinear discrete-time dynamical system is considered to describe the problem explicitly through process and measurement model as illustrated in Figure 2.

The process model of mobile robot in SLAM from time  $k$  to time  $k + 1$  is described as

$$X_{k+1} = FX_k + Bu_k + Gw_k, \quad (2)$$

$$\equiv f(X_k, \omega_k, \nu_k, \delta\omega, \delta\nu), \quad (3)$$

where  $X_k$  is the state of the mobile robot and landmarks as defined in (1),  $u_k = [\omega_k \ \nu_k]^T \in \mathbb{R}^p$  designates the control input, and  $w_k$  is the process noise.  $F \in \mathbb{R}^{(3+2m) \times (3+2m)}$ ,  $B \in \mathbb{R}^{(3+2m) \times (p)}$ , and  $G \in \mathbb{R}^{(3+2m) \times (3+2m)}$  are the state transition matrix, control matrix, and noise covariance matrix, respectively. Since SLAM of a mobile robot is a nonlinear system, process model is defined in a nonlinear form as shown in (3). A model of two-wheel mobile robot (unicycle) is used in this study. Hence, the process model to define the kinematic movement of the mobile robot at time  $k + 1$  is shown as

$$\theta_{k+1} = \theta_k + f_\theta(\omega_k, \nu_k, \delta\omega, \delta\nu), \quad (4)$$

$$x_{k+1} = x_k + (\nu_k + \delta\nu)T \cos(\theta_k), \quad (5)$$

$$y_{k+1} = y_k + (\nu_k + \delta\nu)T \sin(\theta_k), \quad (6)$$

$$X_{m,k+1} = X_{m,k}, \quad (7)$$

where  $\omega_k$  is mobile robot angular acceleration and  $\nu_k$  is its velocity with associated noises,  $\delta\omega$  and  $\delta\nu$ .  $T$  is the sampling rate or the time interval of one movement step. The process model of the landmarks  $X_{m,k+1} = [x_i \ y_i]^T$  for  $i = 1, 2, \dots, l$  is unchanged with zero noise as landmarks are assumed to be stationary, (7). Besides, the data association for SLAM is assumed perfectly given in this study.

During observation, mobile robot makes measurements using its exteroceptive sensors and the measurement model is shown as follows:

$$z_i = \begin{bmatrix} r_i \\ \phi_i \end{bmatrix} = H_i(X_k) + v_{r,\phi_i}, \quad (8)$$

where  $H_i$  is the measurement matrix and  $v_{r,\phi_i}$  is the noise with covariance matrix  $R_k$ .  $H_i(X_k)$  defines that the measurement done by the mobile robot at time  $k$  is linear. However, for a nonlinear system Jacobian transformation of  $H_i$  is required as shown in (16) later. At time  $k + 1$ , the observation of  $i$ th landmark is a range  $r_i$  and bearing  $\phi_i$  which indicates relative distance and angle from mobile robot to any observed landmarks. It is assumed that the sensors on the robot are equipped with a range and bearing sensors that perform the observations of the landmarks in the environment and also encoders at the wheels for the measurement of vehicle speed. Range and bearing are defined as

$$r_i = \sqrt{(y_i - y_{k+1})^2 + (x_i - x_{k+1})^2} + v_{r_i}, \quad (9)$$

$$\phi_i = \arctan\left(\frac{y_i - y_{k+1}}{x_i - x_{k+1}}\right) - \theta_{k+1} + v_{\phi_i},$$

where  $(x_{k+1}, y_{k+1}, \theta_{k+1})$  is current robot position,  $(x_i, y_i)$  is the position of observed landmark, and  $v_{r_i}$  and  $v_{\phi_i}$  are the noises of both distance and angle measurements.

2.2. *H $\infty$  Filter-Based SLAM.* The *H $\infty$*  filter algorithm shows approximately the same structure to the well-known extended Kalman filter (EKF). The presence of  $\gamma$  in the state error covariance owns the essence of *H $\infty$*  filter and acts as the main difference to EKF algorithm. *H $\infty$*  filter theoretically denotes that, for a given  $\gamma > 0$ , the filter attempts to find a solution for an estimated state  $\widehat{X}_k$  that satisfies the following criteria:

$$\gamma > \sup_{X_0, v, w} \frac{\sum_{k=0}^N \|X_k - \widehat{X}_k\|}{\left\{ \|X_0 - \bar{X}_0\|_{P_0}^2 + \sum_{k=0}^N \|v_k\|_{R_k}^2 + \sum_{k=0}^N \|w_k\|_{Q_k}^2 \right\}^{1/2}}, \quad (10)$$

where  $X_0, X_k \in \mathbb{R}^{3+2m}$  is the robot ( $\in \mathbb{R}^3$ ) and landmarks ( $\in \mathbb{R}^{2m}$ ,  $m = 1, 2, \dots, N$ ) states.  $w_k$  and  $v_k$  are the process and measurement noises with covariance of  $Q_k \geq 0$  and  $R_k > 0$ , respectively, and  $P_0 > 0$  is the initial state covariance. The above equation alternatively means that the estimation error to the noise ratio is less than a certain level of  $\gamma$ . This method also assumes that the noise distributions are statistically bounded.

Similar to EKF, the state is predicted based on the system's previous information and then is estimated based on the measurements data obtained from the sensors. In *H $\infty$*  filter algorithm, the prediction step which starts from an initial state is given by

$$\widehat{X}_{k+1}^- = f_k(\widehat{X}_k, \omega_k, \nu_k, 0, 0), \quad (11)$$

where  $\widehat{X}_k \in \mathbb{R}^{(3+2m) \times (3+2m)}$  is the estimated augmented mobile robot and landmarks state with its associated covariance  $P_{k+1}^-$ . The associated state error covariance of the estimation error is given by

$$P_{k+1}^- = \nabla f_r P_k [I_n - \gamma^{-2} P_k + \nabla H_i^T R_k^{-1} \nabla H_i P_k]^{-1} \nabla f_r^T + \nabla g_{\omega\nu} \Sigma_k \nabla g_{\omega\nu}^T, \quad (12)$$

where  $P_k$  is the state error covariance of previous estimation error and  $\Sigma_k$  is the covariance of the control noise  $\delta\omega$  and  $\delta\nu$ . The covariance matrix of the state  $P_k$  is defined in the following subsection.  $\nabla f_r$  and  $\nabla g_{\omega\nu}$  are the Jacobian transformations with respect to the robot position and the process noise, respectively. Those Jacobian transformations are evaluated from the mobile robot motion in (4)–(7) at the current state estimate  $\widehat{X}_k$ . For  $T = 1$  in a case of stationary landmarks, the following are obtained:

$$\nabla f_r = \begin{bmatrix} 1 & 0 & 0 & 0 \\ -\gamma \sin \theta & 1 & 0 & 0 \\ \gamma \cos \theta & 0 & 1 & 0 \\ 0 & 0 & 0 & I_n \end{bmatrix}, \quad (13)$$

$$\nabla g_{\omega\nu} = \begin{bmatrix} f_{\omega\nu\theta} & 0 & 0 & 0 \\ 0 & f_{\omega\nu x} & 0 & 0 \\ 0 & 0 & f_{\omega\nu y} & 0 \\ 0 & 0 & 0 & 0 \end{bmatrix},$$

where  $I_n$  is an identity matrix with an appropriate dimension.  $f_{\omega\nu\theta}$ ,  $f_{\omega\nu x}$ , and  $f_{\omega\nu y}$  define the process noise of the robot motion about its angle and  $x$ ,  $y$  positions, respectively.

The mobile robot continues the process with the observation and measurement using its sensors and this step consequently results in a measurement model as shown in (8). Hence, the mobile robot updates its current location through

$$\widehat{X}_{k+1}^+ = \nabla f_r \widehat{X}_k + K_k (z_{i,k} - \nabla H_i \widehat{X}_k), \quad (14)$$

where the updated state covariance  $P_{k+1}^+$  is given by

$$P_{k+1}^+ = \nabla f_r P_k \psi_k^{-1} \nabla f_r^T + \nabla g_{\omega\nu} \Sigma_k \nabla g_{\omega\nu}^T, \quad (15)$$

where  $\psi = I_n + (\nabla H_i^T R_k^{-1} \nabla H_i - \gamma^{-2} I_n) P_k$  and  $K_k = P_k \nabla H_i^T (\nabla H_i P_k \nabla H_i^T + R_k)^{-1}$ . Since SLAM is a nonlinear system, the Jacobian transformation of measurement between mobile robot position and any  $i$ th landmark results in the following function  $\nabla H_i$ :

$$\nabla H_i = \begin{bmatrix} 0 & -\frac{dx}{r} & -\frac{dy}{r} & \frac{dx}{r} & \frac{dy}{r} \\ \frac{r}{r^2} & \frac{r}{r^2} & -\frac{dx}{r^2} & -\frac{dy}{r^2} & \frac{dx}{r^2} \\ -1 & \frac{dy}{r^2} & -\frac{dx}{r^2} & -\frac{dy}{r^2} & \frac{dx}{r^2} \end{bmatrix}, \quad (16)$$

where

$$dx = x_i - x_k, \quad (17)$$

$$dy = y_i - y_k, \quad (17)$$

$$r = \sqrt{dx^2 + dy^2}.$$

2.3. *State Error Covariance Matrix.* The covariance matrix of a state estimation in SLAM is a combination matrix of mobile robot and landmark position covariance matrices and correlation between mobile robot and landmarks. Correlations between mobile robot position and landmarks estimation arise when the measurements are incorporated and thus the state error covariance becomes dense. The state error covariance  $P_k$  is defined generally as

$$P_k = \begin{bmatrix} P_{vv} & P_{vm} \\ P_{vm}^T & P_{mm} \end{bmatrix}, \quad (18)$$

where  $P_{vv}$  is the covariance matrix of the robot position,  $P_{mm}$  is the covariance matrix of the landmark position, and  $P_{vm}$  is cross-covariance matrix of the robot and landmark position or cross-correlation between them.

The dimension of state error covariance in SLAM is  $(3 + 2m) \times (3 + 2m)$ . The size of covariance matrix will grow as the robot continuously observed new landmarks in the environment. State error covariance for SLAM is fully represented in (19). The state error covariance indicates the error associated with the robot and landmark state estimations. From the state error covariance, the increment or decrement of uncertainties and errors of the estimation could be observed, which represent the precision and consistency of the estimation. Therefore, the study on the behaviour of state error covariance is one of the important issues in designing the technique of mobile robot SLAM:

$$\begin{bmatrix}
 P_{\theta\theta} & P_{\theta x} & P_{\theta y} & P_{\theta m_{1,x}} & P_{\theta m_{1,y}} & \cdots & \cdots & P_{\theta m_{n,x}} & P_{\theta m_{n,y}} \\
 P_{x\theta} & P_{xx} & P_{xy} & P_{xm_{1,x}} & P_{xm_{1,y}} & \cdots & \cdots & P_{xm_{n,x}} & P_{xm_{n,y}} \\
 P_{y\theta} & P_{yx} & P_{yy} & P_{ym_{1,x}} & P_{ym_{1,y}} & \cdots & \cdots & P_{ym_{n,x}} & P_{ym_{n,y}} \\
 P_{m_{1,x}\theta} & P_{m_{1,x}x} & P_{m_{1,x}y} & P_{m_{1,x}m_{1,x}} & P_{m_{1,x}m_{1,y}} & \cdots & \cdots & P_{m_{1,x}m_{n,x}} & P_{m_{1,x}m_{n,y}} \\
 P_{m_{1,y}\theta} & P_{m_{1,y}x} & P_{m_{1,y}y} & P_{m_{1,y}m_{1,x}} & P_{m_{1,y}m_{1,y}} & \cdots & \cdots & P_{m_{1,y}m_{n,x}} & P_{m_{1,y}m_{n,y}} \\
 \vdots & \vdots & \vdots & \vdots & \vdots & \cdots & \cdots & \vdots & \vdots \\
 \vdots & \vdots & \vdots & \vdots & \vdots & \cdots & \cdots & \vdots & \vdots \\
 P_{m_{n,x}\theta} & P_{m_{n,x}x} & P_{m_{n,x}y} & P_{m_{n,x}m_{1,x}} & P_{m_{n,x}m_{1,y}} & \cdots & \cdots & P_{m_{n,x}m_{n,x}} & P_{m_{n,x}m_{n,y}} \\
 P_{m_{n,y}\theta} & P_{m_{n,y}x} & P_{m_{n,y}y} & P_{m_{n,y}m_{1,x}} & P_{m_{n,y}m_{1,y}} & \cdots & \cdots & P_{m_{n,y}m_{n,x}} & P_{m_{n,y}m_{n,y}}
 \end{bmatrix}. \quad (19)$$

### 3. Conditions for Convergence in $H_\infty$ Filter-Based SLAM

$H_\infty$  filter algorithm has a significant effect on its performance. Unlike the EKF,  $\gamma$  appears in the prediction and update process; therefore, it requires additional attention from the designer to design their system appropriately. The presence of  $\gamma$  acts as an attenuator to reduce the system uncertainties during mobile robot observation and can be adjustable by applying  $\gamma$ -switching technique [30]. However, in this study,  $\gamma$  is fixed as the purpose of the study is to find the sufficient conditions for a constant  $\gamma$ . If  $\gamma$  continuously changes, the result would approximate Kalman filter behaviour. Therefore, the results obtained may exhibit almost the same performance as the Kalman filter which is deemed unsuitable for this study.

Based on  $H_\infty$  filter algorithm, the estimated state error covariance equation (15) can be simplified as

$$P_{k+1} = P_k + Q_k. \quad (20)$$

Equation (20) shows that, in every update, the existence of process noise  $Q_k$  has a significant effect on the state error covariance. The equation is also one of the factors that provide sufficient information in  $H_\infty$  filter. Thus,  $H_\infty$  filter is sensitive to the initial state covariance, process, and measurement noises distributions as reported in the literature [25]. Taking into account these variables, the analysis contributes adequately to explaining the filter performance and consistency. As the  $H_\infty$  filter-based SLAM is still considered as a new technique discovered for SLAM, no analytical results of convergence are available. Therefore, a theoretical study about  $H_\infty$  filter convergence is essential.

Motivated by the aforementioned research gap, this study attempts to clarify the effect of initial condition of state covariance with the influence of process and measurement noise distributions on the  $H_\infty$  filter behaviour in SLAM. Two case studies have been defined for the study.

- (1) Robot initial state error covariance is smaller than the landmarks initial state error covariance such that  $P_{0vv} \ll P_{0mm}$ .

- (2) Robot initial state error covariance is big and the same as the landmarks initial state error covariance such that  $P_{0vv} = P_{0mm}$ .

The first case defines that the robot has more confidence about its location than the landmark. This case relies on the assumption that robot has an efficient proprioceptive sensors for sensory purposes. Next, the second case defines that both robot and landmarks initial state error covariances are unknown. Generally, this case is more alike to the problem in real SLAM application as usually no prior information is available for reference. Provided by these two conditions, a theoretical study and analysis are suggested to comprehend their influences on SLAM problem. Parallel to the proposed cases, this study also investigates the consequences of process and measurement noises to the estimation.

As remarked in the literature, the performance of  $H_\infty$  filter is sensitive and depends on the design parameters such as the process and measurement noises and also the initial state error covariance. The study continues to describe explicitly that the selection of design parameters should satisfy some conditions to guarantee  $H_\infty$  filter surpassing EKF performance (see [27]). Furthermore, there are certain trade-offs which are necessary between the design parameters to achieve the best solution in  $H_\infty$  filter-based SLAM.

*Definition 1.* The Jacobian matrix when a mobile robot observes only one new landmark in its surrounding at point A and makes  $n$  observations is given by [19]

$$\nabla H_A = \begin{bmatrix}
 0 & -\frac{dx_A}{r_A} & -\frac{dy_A}{r_A} & \frac{dx_A}{r_A} & \frac{dy_A}{r_A} \\
 -1 & \frac{dy_A}{r_A^2} & -\frac{dx_A}{r_A^2} & -\frac{dy_A}{r_A^2} & \frac{dx_A}{r_A^2}
 \end{bmatrix} = [-e \quad -A \quad A], \quad (21)$$

where

$$e = \begin{bmatrix} 0 \\ 1 \end{bmatrix}, \quad A = \begin{bmatrix} \frac{dx_A}{r_A} & \frac{dy_A}{r_A} \\ -\frac{dy_A}{r_A^2} & \frac{dx_A}{r_A^2} \end{bmatrix} \quad (22)$$

evaluated at the true landmark  $(x_m, y_m)$  and the true robot position  $(x_A, y_A)$  and its elements are defined by

$$\begin{aligned} dx_A &= x_m - x_A, \\ dy_A &= y_m - y_A, \\ r_A &= \sqrt{dx_A^2 + dy_A^2}. \end{aligned} \quad (23)$$

The aforementioned definition will be excessively used in this study.

*Definition 2.* The state vector of mobile robot and landmarks location (1)  $X_k$  follows a Gaussian distribution in which it is represented through a mean and covariance of its elements:

$$X_k \sim N(x, P). \quad (24)$$

The covariance indicates the level of certainty of the mean estimation; the larger the covariance, the larger the uncertainty of the state estimation. Fisher information matrix (FIM)  $\Omega$  specifies the weight of information contained in a Gaussian distribution. In the case of mobile robot SLAM, FIM indicates the information obtained by the mobile robot from each observation. FIM is the inverse of the state error covariance. The information obtained is inversely proportional to the uncertainty:

$$\Omega_k = P_k^{-1}. \quad (25)$$

Fisher information matrix at time  $k + 1$  is the summation of information matrix at time  $k$  and the new information obtained from the observation, described as follows [19]:

$$\Omega_{k+1} = \Omega_k + \nabla H_i^T R_k \nabla H_i. \quad (26)$$

The Fisher information matrix is used to determine the updated state error covariance for each update in this study. If the mobile robot starts moving from its initial position to point A and makes an observation at that point, then with respect to Definitions 1 and 2, the FIM yields the following equation:

$$\begin{aligned} \Omega_{k+1} &= \begin{bmatrix} P_{0vv} & 0 \\ 0 & P_{0mm} \end{bmatrix}^{-1} + \begin{bmatrix} -H_A^T \\ A^T \end{bmatrix} R_A^{-1} \begin{bmatrix} -H_A & A \end{bmatrix} - \gamma^{-2} I_n \\ &= \begin{bmatrix} P_{0vv}^{-1} + H_A^T R_A^{-1} H_A - \gamma^{-2} I_n & -H_A^T R_A^{-1} A \\ -A^T R_A^{-1} H_A & P_{0mm}^{-1} + A^T R_A^{-1} A - \gamma^{-2} I_n \end{bmatrix}, \end{aligned} \quad (27)$$

with  $H_A = [e \ A]$  and thus from (21)  $\nabla H_A = [-H_A \ A]$ .  $P_{0vv}$  and  $P_{0mm}$  are the initial state error covariance for robot and landmarks, respectively. The landmarks are assumed to be stationary, and hence there are no noises affecting the prediction process for landmarks state. Equation (27) is claimed as the feasible condition [31]. This condition is very important as it defines the amount of information available at that specific time.

Before presenting the main results, the feasibility conditions for  $H\infty$  filter-based SLAM are proposed.

**Theorem 3.** *With the consideration of (4)–(7) and (12), the solution of the filter exists if it satisfies the feasibility conditions of  $\gamma$  for each case as stated below:*

- (1) if  $P_0 \gg R$ , then  $\gamma^2 > R$ ;
- (2) if  $P_0 < R$ , then  $\gamma^2 > P_0$ .

*Proof.* The feasibility conditions are analysed separately for each case. To reveal these criteria clearly, consider a one-dimensional SLAM (1D SLAM) problem, that is, a robot with a single coordinate system observing landmarks. Given that for all conditions  $P_0 > 0$  and  $\gamma > 0$ ,

- (1) if  $P_0 \gg R_A$ , then  $\gamma^2 > R_A$ .

To ensure convergency, the covariance matrix should possess positive semidefinite (PSD) matrix properties of its elements [28]. Since  $\Omega = P^{-1}$  and  $P_0 \gg R$ , the first element of (27) has the following criteria:

$$H_A^T R_A^{-1} H_A - \gamma^{-2} > P_0^{-1}. \quad (28)$$

Note that the left and right hand sides of (28) still exhibit a positive semidefinite matrix. Examining the case for 1D SLAM, the following equation is achieved:

$$R_A^{-1} - \gamma^{-2} > P_0^{-1}. \quad (29)$$

Using this new proposed condition and considering that the updated information must be at least a PSD matrix,

$$\begin{aligned} R_A^{-1} - \gamma^{-2} &> 0, \\ R_A^{-1} &> \gamma^{-2}, \\ \gamma^2 &> R_A. \end{aligned} \quad (30)$$

- (2) If  $P_0 < R_A$ , then  $\gamma^2 > P_0$ .

Similar to the analysis of case (1), the first element of FIM is examined to find the consequences of  $P_0 < R_A$ . Under the same assumption of PSD characteristics as in (1), the following results are obtained:

$$P_0^{-1} + H_A^T R_A^{-1} H_A - \gamma^{-2} > P_0^{-1} - \gamma^{-2} > 0. \quad (31)$$

Hence, for 1D SLAM,

$$\begin{aligned} \gamma^{-2} &< P_0^{-1}, \\ \gamma^2 &> P_0. \end{aligned} \quad (32)$$

Based on the proposed Theorem 3, additional conditions are required prior to implementation stage to ensure that  $H\infty$  filter estimation is converging. Besides, the results have aided the previous findings significantly which are identified by [31]. Remark that the initial state covariances for mobile robot and landmarks are considered similar in Theorem 3. Now we have the appropriate conditions and therefore we are ready to examine the sufficient conditions for  $H\infty$  filter-based SLAM convergence of each case as defined previously.  $\square$

3.1. Case 1:  $P_{0vv} \ll P_{0mm}$ . The preceding section explains that FIM is used to interpret  $H\infty$  filter behaviour in each update. Since the main difference between  $H\infty$  filter and Kalman filter is due to the existence of  $\gamma$  for which the characteristics can be explicitly recognized by (27), the equation may aid in analysing its significance and influence of design parameters on  $H\infty$  filter performance.

If  $P_{0vv} \ll P_{0mm}$ , then the landmarks have high uncertainties. Thus, it is appropriate to assume that  $P_{0mm}^{-1} \rightarrow 0$ . By this assumption, FIM can be expressed as follows:

$$\Omega_{k+1} = \begin{bmatrix} P_{0vv}^{-1} + H_A^T R_A^{-1} H_A - \gamma^{-2} I_n & -H_A^T R_A^{-1} A \\ -A^T R_A^{-1} H_A & A^T R_A^{-1} A - \gamma^{-2} I_n \end{bmatrix}. \quad (33)$$

Notice that the diagonal elements are the essential elements for the designer to obtain some sufficient conditions in  $H\infty$  filter. This is because each variable occupies mobile robot and landmarks uncertainties. Hence, smaller values of these variables are being demanded to achieve better state estimation. Moreover,  $\Omega$  must always preserve at least a positive semidefinite matrix in every observation. These two facts are necessary conditions to secure a reliable estimation in  $H\infty$  filter-based SLAM. To illustrate this matter clearly, the following proposition is presented. Let  $P_{0vv(x)}$ ,  $P_{0vv(y)}$ , and  $P_{0vv(\theta)}$  define  $x$ ,  $y$ ,  $\theta$  robot initial state covariances.

**Proposition 4.** For  $\gamma > 0$ , in a case of a robot that has more confidence about its initial state than the landmarks state,  $\gamma$  selection is affected by the initial state covariance, process, and measurement noises and its selection must satisfy the following properties:

$$\begin{aligned} \gamma &> \sqrt{\frac{1}{P_{0vv(\theta)}^{-1} + R_A^{-1}}}, \\ \gamma &> \sqrt{\frac{R_A(dx^2 + dy^2)^2}{(P_{0vv(x)} + \Sigma_x)^{-1} R_A(dx^2 + dy^2)^2 + dx^4 + dx^2 dy^2 + dy^2}}, \\ \gamma &> \sqrt{\frac{R_A(dx^2 + dy^2)^2}{(P_{0vv(y)} + \Sigma_y)^{-1} R_A(dx^2 + dy^2)^2 + dy^4 + dy^2 dx^2 + dx^2}}, \end{aligned} \quad (34)$$

where  $\Sigma_x$  and  $\Sigma_y$  are the associated process noise covariance for robot  $x$ ,  $y$  coordinate.

*Proof.* First the diagonal elements are analysed. This consequently led us to determine both robot and landmarks information during robot observations which are represented by  $P_{0vv}^{-1} + H_A^T R_A^{-1} H_A - \gamma^{-2} I_n$  and  $A^T R_A^{-1} A - \gamma^{-2} I_n$ . The former

equation can substantially explain the latter equation. This is shown by the following calculations:

$$\begin{aligned} &P_{0vv}^{-1} + H_A^T R_A^{-1} H_A - \gamma^{-2} I_n \\ &= \begin{bmatrix} P_{0vv(\theta)}^{-1} & 0 \\ 0 & P_{0vv(xy)}^{-1} \end{bmatrix} + \begin{bmatrix} e^T \\ A^T \end{bmatrix} R_A^{-1} \begin{bmatrix} e & A \end{bmatrix} - \gamma^{-2} I_n \\ &= \begin{bmatrix} P_{0vv(\theta)}^{-1} + e^T R_A^{-1} e - \gamma^{-2} I_n & e^T R_A^{-1} A \\ A^T R_A^{-1} e & P_{0vv(xy)}^{-1} + A^T R_A^{-1} A - \gamma^{-2} I_n \end{bmatrix}, \end{aligned} \quad (35)$$

where  $P_{0vv(\theta)}$  and  $P_{0vv(xy)}$  are the initial robot state error covariance about its angle and  $x$ ,  $y$  position, respectively. Note that both diagonal elements must preserve PSD in each observation. In SLAM, mobile robot heading angle acts as the primary factors that determine consistency in SLAM [19]. Hence, it should be analysed differently with other elements of the state error covariance. As each diagonal matrix element must at least possess a PSD, then, for the robot heading angle covariance  $P_{0vv(\theta)}$ , the following characteristics are compulsory:

$$\begin{aligned} &P_{0vv(\theta)}^{-1} + R_A^{-1} - \gamma^{-2} > 0, \\ &\gamma^2 > \frac{1}{P_{0vv(\theta)}^{-1} + R_A^{-1}}. \end{aligned} \quad (36)$$

Now, the analysis proceeds for the robot and landmarks states about its  $x$ ,  $y$  estimations, that is, the second diagonal element. By utilizing Definition 1 and (27) being referred,

$$\begin{aligned} &A^T R_A^{-1} A \\ &= \begin{bmatrix} \frac{dx_A}{r_A} & -\frac{dy_A}{r_A^2} \\ \frac{dy_A}{r_A} & \frac{dx_A}{r_A^2} \end{bmatrix} R_A^{-1} \begin{bmatrix} \frac{dx_A}{r_A} & \frac{dy_A}{r_A} \\ -\frac{dy_A}{r_A^2} & \frac{dx_A}{r_A^2} \end{bmatrix} \\ &= \begin{bmatrix} \left(\frac{dx_A^2}{r_A^2} + \frac{dy_A^2}{r_A^4}\right) R_A^{-1} & \left(\frac{dx_A dy_A}{r_A^2} - \frac{dy_A dx_A}{r_A^4}\right) R_A^{-1} \\ \left(\frac{dy_A dx_A}{r_A^2} - \frac{dx_A dy_A}{r_A^4}\right) R_A^{-1} & \left(\frac{dy_A^2}{r_A^2} + \frac{dx_A^2}{r_A^4}\right) R_A^{-1} \end{bmatrix}. \end{aligned} \quad (37)$$

Based on this case, it is configurable that the robot has some degree of confidence about its initial location compared to landmarks condition which consists of very large initial state covariance. Hence, the inverse of the landmarks initial state covariance is approximating zero. Substituting (37) into the second diagonal term of (35) appropriately leads to the following expression:

$$\begin{aligned} &P_{0vv(x)}^{-1} + \left(\frac{dx_A^2}{r_A^2} + \frac{dy_A^2}{r_A^4}\right) R_A^{-1} - \gamma^{-2} > 0, \\ &P_{0vv(y)}^{-1} + \left(\frac{dy_A^2}{r_A^2} + \frac{dx_A^2}{r_A^4}\right) R_A^{-1} - \gamma^{-2} > 0. \end{aligned} \quad (38)$$

By simple algebraic rearrangement to determine  $\gamma$  sufficient conditions, the following is proposed to obtain better estimation result:

$$\begin{aligned} \gamma^2 &> \frac{R_A(dx_A^2 + dy_A^2)^2}{P_{0vv}^{-1}R_A(dx_A^2 + dy_A^2)^2 + dx_A^4 + dx_A^2dy_A^2 + dy_A^2}, \\ \gamma^2 &> \frac{R_A(dx_A^2 + dy_A^2)^2}{P_{0vv}^{-1}R_A(dx_A^2 + dy_A^2)^2 + dy_A^4 + dy_A^2dx_A^2 + dx_A^2}. \end{aligned} \quad (39)$$

This result significantly describes that it is difficult to obtain an appropriate  $\gamma$  due to the nonlinear characteristics of robot movement and noises. Nevertheless, the prediction step also embraces the process noise (refer to (20)); it is found that bigger process noise required bigger  $\gamma$ . Next, the PSD characteristic is examined in each FIM update. It was found that FIM, which behaves as the information during observations has provided a proper selection of  $\gamma$  to avoid finite escape time phenomena.  $\square$

**Theorem 5.** *Note that  $\gamma > 0$  and Theorem 3 is satisfied. If the mobile robot initial state covariance is very small compared to the initial state covariance of landmarks, then  $\gamma$  is chosen to satisfy the following equations:*

- (1)  $\gamma > \sqrt{R}$ ,
- (2)  $\gamma > \sqrt{P_{0vv}}$ .

*If else, the updated state error covariance exhibits finite escape time.*

*Proof.* From the properties of PSD, the determinant of the matrix must be nonnegative. This behaviour is necessary in probabilistic SLAM. As a matter of fact, this criterion is used to obtain some typical features for  $\gamma$  selection. The determinant of (33) gives

$$\begin{aligned} &(P_{0vv}^{-1} + H_A^T R_A^{-1} H_A - \gamma^{-2} I_n) (A^T R_A^{-1} A - \gamma^{-2} I_n) \\ &- (H_A^T R_A^{-1} A A^T R_A^{-1} H_A) > 0. \end{aligned} \quad (40)$$

However, the above nonlinear equation is difficult to explain the effect of  $\gamma$  for every respective update. We propose the analysis in linear 1D SLAM to visualize how  $\gamma$  influences the estimation. In 1D SLAM, the determinant eventually becomes as follows:

$$\begin{aligned} &(P_{0vv}^{-1} + R_A^{-1} - \gamma^{-2}) (R_A^{-1} - \gamma^{-2}) - R_A^{-2} > 0, \\ &P_{0vv}^{-1} R_A^{-1} - \gamma^{-2} P_{0vv}^{-1} - 2\gamma^{-2} R_A^{-1} + \gamma^{-4} > 0, \\ &\gamma^{-4} - (P_{0vv}^{-1} + 2R_A^{-1}) \gamma^{-2} + P_{0vv}^{-1} R_A^{-1} > 0, \end{aligned} \quad (41)$$

where  $H_A = [-1 \ 1]$  and  $A = 1$ . Furthermore, it is easily recognized that as  $P_{0vv}, R_A > 0$ , then the following are achieved:

$$\begin{aligned} &\gamma^{-4} - (P_{0vv}^{-1} + 2R_A^{-1}) \gamma^{-2} + P_{0vv}^{-1} R_A^{-1} \\ &< \gamma^{-4} - (P_{0vv}^{-1} + R_A^{-1}) \gamma^{-2} + P_{0vv}^{-1} R_A^{-1}, \end{aligned} \quad (42)$$

$$\begin{aligned} &\gamma^{-4} - (P_{0vv}^{-1} + R_A^{-1}) \gamma^{-2} + P_{0vv}^{-1} R_A^{-1} \\ &= (\gamma^{-2} - P_{0vv}^{-1}) (\gamma^{-2} - R_A^{-1}), \\ &(\gamma^{-2} - P_{0vv}^{-1}) (\gamma^{-2} - R_A^{-1}) > 0. \end{aligned} \quad (43)$$

Hence, there exist two different cases with two respective conditions to fulfil (43).

- (1)  $\gamma > \sqrt{R_A}$  and  $\gamma > \sqrt{P_{0vv}}$ .
- (2)  $\gamma < \sqrt{R_A}$  and  $\gamma < \sqrt{P_{0vv}}$ .

However, the above condition (2) is unlikely to happen. This is related to (27) where this condition can yield a negative definite matrix. Therefore, condition (1) is apparently the only solution for this case. Moreover, from the above analysis it explicitly identifies the relationship between  $\gamma$ , initial state covariance, and measurement noise. In addition, the process noise covariance is also influencing  $\gamma$  selection as it is included in the state error covariance prediction step.

As defined above, the results consistently show the same behaviour as Theorem 3 in which  $\gamma$  must be selected properly considering the environment and system situations; whenever the initial state error covariance for mobile robot  $P_{0vv}$  is much smaller than landmarks covariance  $P_{0mm}$ , then  $\gamma$  must be designed according to these two conditions. Note that Theorem 5 describes a case where the initial state covariance between mobile robot and landmarks is different, whereas Theorem 3 only considers that both initial state covariances have the same values. Furthermore, both feasible conditions proposed by Theorem 3 must be satisfied for this case.

Moreover, in navigation of mobile robot, the heading angle of mobile robot acts as an important factor to be considered in SLAM [19]. As been proposed by Theorem 3 and Proposition 4, the designer must ensure that those feasibility conditions and (36) are fulfilled to successfully implement the filter approach in their application.  $\gamma$  is selected by incrementally increasing its value with regards to the value defined in Theorem 3 and Proposition 4 to obtain the best solution.  $\square$

**3.2. Case 2:  $P_{0vv} = P_{0mm}$ .** This condition is the appropriate situation of an actual SLAM problem. It is obvious that if a robot is arbitrarily put in an unknown environment, then it should not have information about its initial location even though it is being equipped with high accuracy sensors. Such a situation presumes a uniform distribution for both robot and landmarks belief where both initial state covariances yield very big uncertainties. The following theorem is proposed to indicate  $H_\infty$  filter-based SLAM behaviour for this respective case.



**Theorem 6.** Consider that  $\gamma > 0$  and Theorem 3 is satisfied. There is a  $\gamma$  that gives the best solution to SLAM which satisfies the following, if and only if both robot and landmarks initial state covariances are very big such that robot does not have any prior information about its initial position:

$$\gamma > \sqrt{\frac{R}{2}}. \quad (44)$$

*Proof.* Assume that both robot and landmarks initial state covariances are too big. By referring to the previous case, the determinant of the updated Fisher information matrix for a robot observing landmarks at point A yields the following:

$$\begin{aligned} & (P_{0vv}^{-1} + H_A^T R_A^{-1} H_A - \gamma^{-2} I_n) (P_{0mm}^{-1} + A^T R_A^{-1} A - \gamma^{-2} I_n) \\ & - (H_A^T R_A^{-1} A A^T R_A^{-1} H_A) > 0. \end{aligned} \quad (45)$$

To simplify this analysis, we consider again 1D SLAM problem. We know initially that in this case  $P_{0vv} = P_{0mm} = P_0$  and both initial state covariances are very big. By this assumption and similar steps as (41)–(43), (45) leads us to the following equation:

$$\begin{aligned} & (P_0^{-1} + R_A^{-1} - \gamma^{-2})^2 - R_A^{-2} > 0, \\ & \gamma^{-4} - 2\gamma^{-2} (P_0^{-1} + R_A^{-1}) + P_0^{-2} + 2P_0^{-1} R_A^{-1} > 0. \end{aligned} \quad (46)$$

Consider the above equation and the fact that  $P_0 \gg 0$  and thus  $(P_0^{-1} \rightarrow 0)$ . Hence, through factorization, the following equation is obtained:

$$\begin{aligned} & \gamma^{-4} - 2R_A^{-1} \gamma^{-2} > 0, \\ & \gamma^{-2} (\gamma^{-2} - 2R_A^{-1}) > 0. \end{aligned} \quad (47)$$

Since in  $H\infty$  filter algorithm  $\gamma > 0$ , thus from (47) it appears that the left hand side variables should yield positive values to ensure that the solution of the estimation is available. Therefore, the following relation of  $\gamma$  and measurement noise is obtained:

$$\begin{aligned} & \gamma^{-2} - 2R_A^{-1} > 0, \\ & \gamma > \sqrt{\frac{R_A}{2}}. \end{aligned} \quad (48)$$

It is worth mentioning that the process noise still slightly affects the estimation if it is too big. If such conditions occurred, then  $\gamma$  must be tuned carefully to achieve a desired estimation result. Referring back to the filter algorithm,  $H\infty$  filter estimation should be the same as EKF if  $\gamma$  is set to be very big. Related to this fact, we propose a condition of  $\gamma$  where  $H\infty$  filter has better performance than EKF. If finite escape time is observable, then  $\gamma$  must be tuned by incrementally increasing its value to obtain better result. This is the common step in  $H\infty$  filtering thus finally approximating the same estimation behaviour to EKF. The next section identifies and evaluates our theoretical results.  $\square$

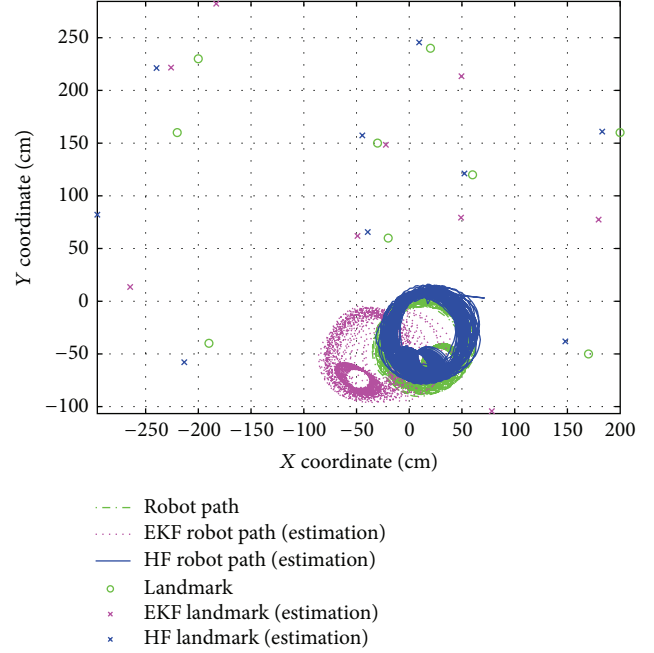


FIGURE 3: Feasibility condition 1: robot localization and map building performance between  $H\infty$  filter and EKF.

## 4. Simulation Results

The proposed theoretical results obtained above are examined through a series of simulations. A small environment which has the parameters as described in Table 1 is considered. It is assumed that the robot exteroceptive sensors can observe their surrounding in a specific range and the process noises are small such that they can be neglected. The robot is assigned to move in some directions while doing its observations. Landmarks are also assumed to be point landmarks, stationary, and situated randomly. Comparison between  $H\infty$  filter- and EKF-based SLAM regarding map construction analysis, state error covariance update, and root-mean-square error (RMSE) evaluation is given for each case that has been analysed in the preceding section. Note that the process noises are kept consistently very small for both cases.

Figures 3 and 4 illustrate the simulation results for the proposed feasibility condition stated by Theorem 3. To evaluate the reliability of the proposed feasibility conditions, the parameters in Table 1 are selected such that they satisfy the defined conditions. Figure 3 demonstrates the results of estimation between  $H\infty$  filter (HF) and extended Kalman filter (EKF) for feasibility condition 1 where condition of  $P_0 \gg R$  is being considered. As illustrated in the figure, HF shows better performance than EKF about the mobile robot and landmarks positions.

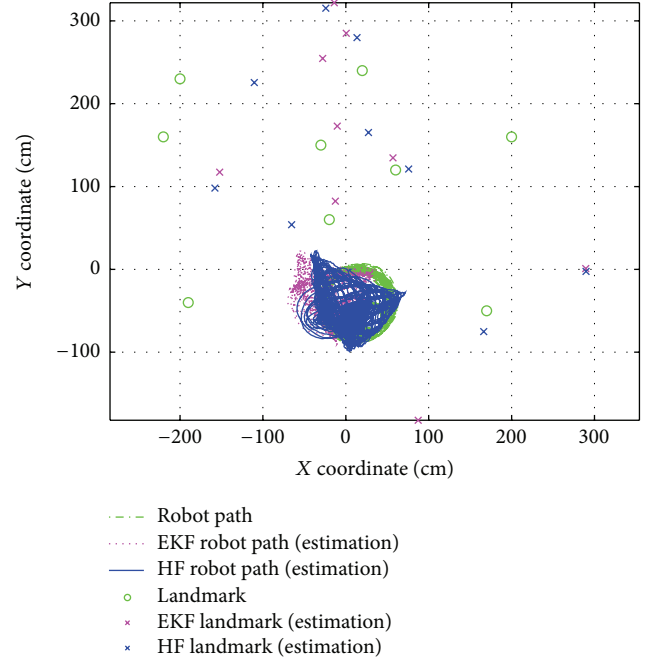
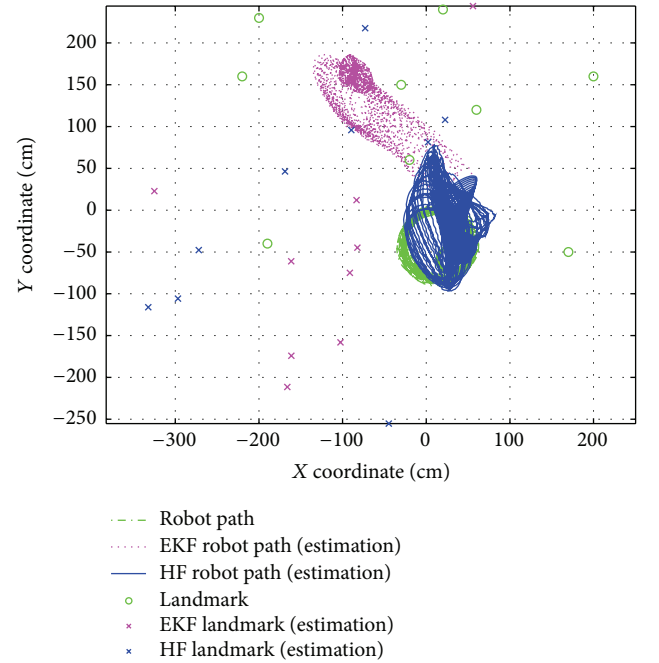
The analysis for feasible condition 2 is depicted in Figure 4. Based on the given figure, if the parameters selected correspond to the described condition, that is,  $P_0 < R$ , then the  $H\infty$  estimation exhibits better performance than EKF. According to these results, if both of the feasible conditions

TABLE I: Simulation parameters.

Sampling time [s]	$T$	0.1
Process noise	$Q_k$	$1 \times 10^{-7}$
Feasibility condition		
Feasibility condition 1		
Robot and landmark initial state covariance	$P_{0vv}$	10
	$P_{0mm}$	10
Measurement noises	$R_{k\theta}$	0.002
	$R_{k(\text{distance})}$	0.002
Selection of Gamma	$\gamma$	0.85
Feasibility condition 2		
Robot and landmark initial state covariance	$P_{0vv}$	2
	$P_{0mm}$	2
Measurement noises	$R_{k\theta}$	5
	$R_{k(\text{distance})}$	5
Selection of Gamma	$\gamma$	2.35
Case analysis		
Case 1		
Robot and landmark initial state covariance	$P_{0vv}$	2
	$P_{0mm}$	20
Measurement noises	$R_{k\theta}$	2
	$R_{k(\text{distance})}$	2
Selection of Gamma	$\gamma$	2
Case 2		
Robot and landmark initial state covariance	$P_{0vv}$	5
	$P_{0mm}$	5
Measurement noises	$R_{k\theta}$	2
	$R_{k(\text{distance})}$	2
Selection of Gamma	$\gamma$	2

are not satisfied, then the estimation diverges and exhibits erroneous results. Besides, the estimation emphasised that finite escape time easily occurred during mobile robot observation. These results can be found in [28].

Figures 5–7 illustrate the simulation results for case 1 whenever the mobile robot has more confidence about its initial position in comparison to the landmarks state covariance; that is,  $P_{0vv} \ll P_{0mm}$ . Based on these figures, it is observed that the estimation of  $H\infty$  filter outperforms EKF. Figure 5 depicts the result of mapping for both filters, while the state error covariances for the estimations are presented in Figure 6. RMSE evaluations of the landmarks estimations are presented in Figure 7. The mobile robot path estimation as well as the estimation of landmarks position in Figure 5 consistently shows that  $H\infty$  filter provides better estimation than EKF. Figure 5 depicts clearly the erroneous estimation of EKF through the path of the mobile robot. The findings can be demonstrated clearly by Figure 6 in which the state error covariance of EKF has higher value than  $H\infty$  filter for both mobile robot and landmarks position. This denotes that the estimation through EKF possesses higher uncertainties under the conditions described by case 1. Based on the RMSE

FIGURE 4: Feasibility condition 2: robot localization and map building performance between  $H\infty$  filter and EKF.FIGURE 5: Case 1: map construction performance between  $H\infty$  filter and EKF.

evaluation for the landmarks position in Figure 7,  $H\infty$  filter also suggests that it has smaller error than EKF. However, these results can only be available if and only if the condition of  $\gamma > \sqrt{R}$  has been satisfied.

Figures 8–10 illustrate the results of case 2 of initial covariances of  $P_{0vv} = P_{0mm} = 5$  for both robot and landmarks

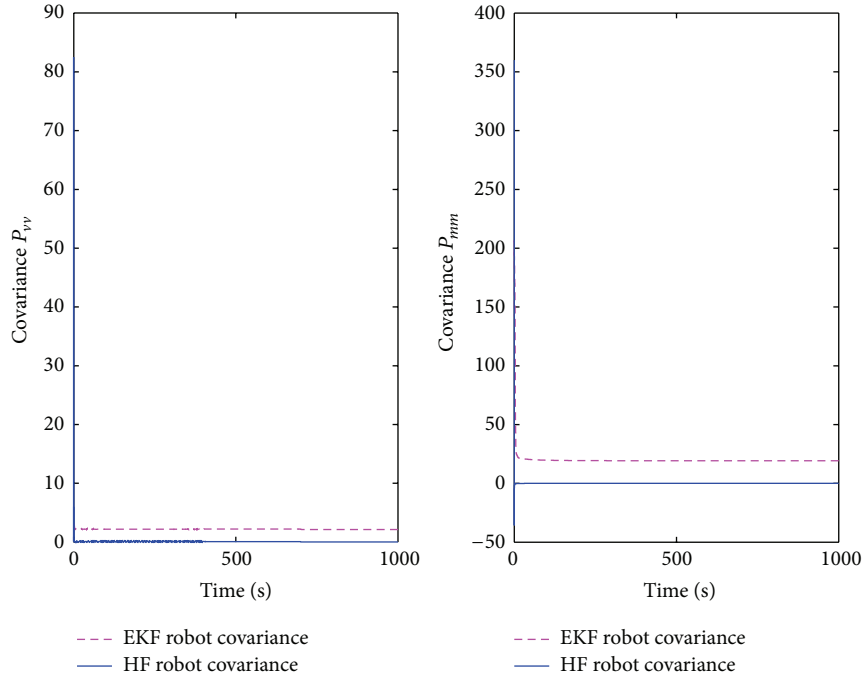


FIGURE 6: Case 1: state error covariance performance between  $H_{\infty}$  filter and EKF.

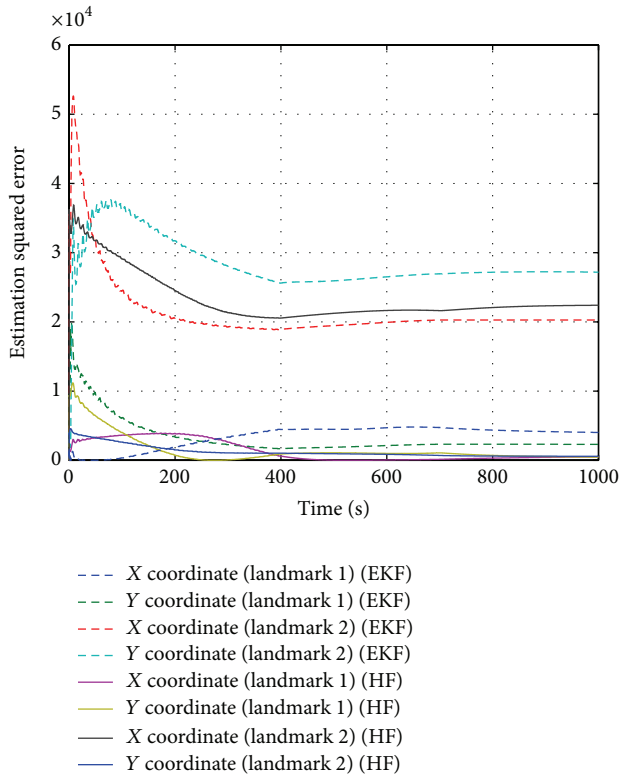


FIGURE 7: Case 1: RMSE performance between  $H_{\infty}$  filter and EKF.

states. A similar performance is observed as described in Figures 5–7. The robot could estimate its current path and location with some level of certainty. The uncertainties

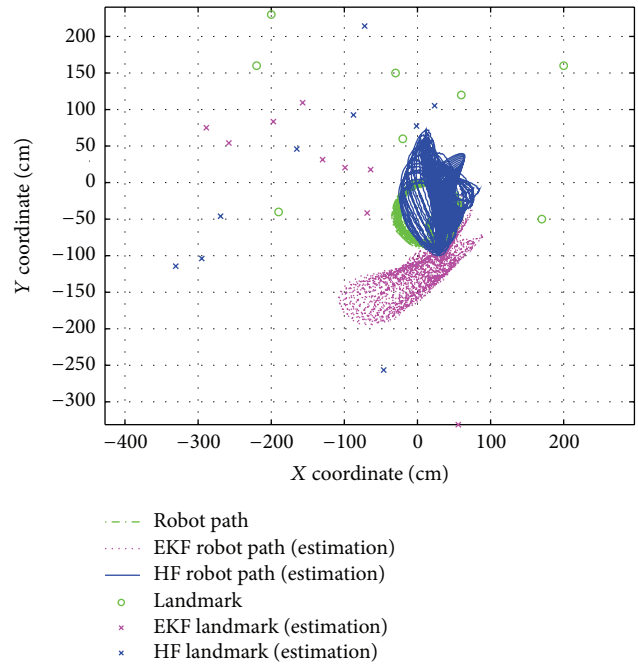


FIGURE 8: Case 2: Map construction performance between  $H_{\infty}$  filter and EKF.

of estimation proved that  $H_{\infty}$  filter still surpasses EKF performance as shown in Figure 9. Moreover, it can be observed from Figure 10, that the RMSE evaluation of the landmarks position has similar characteristics to that of the case 1 (Figure 7). This shows that  $H_{\infty}$  filter can provide a better solution in SLAM problem, if and only if Theorem 6

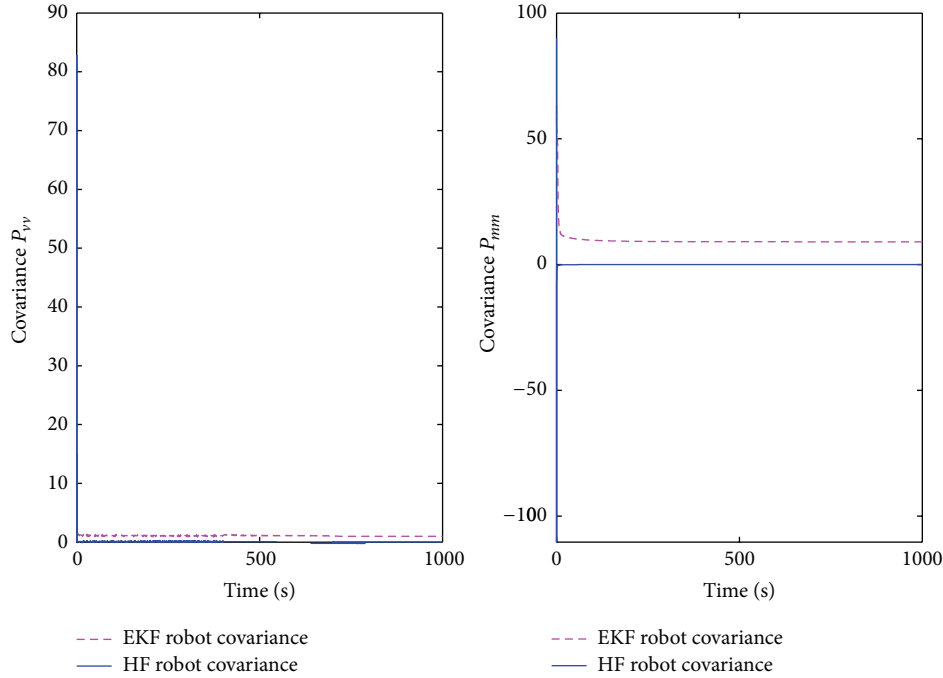


FIGURE 9: Case 2: state error covariance performance between  $H_\infty$  filter and EKF.

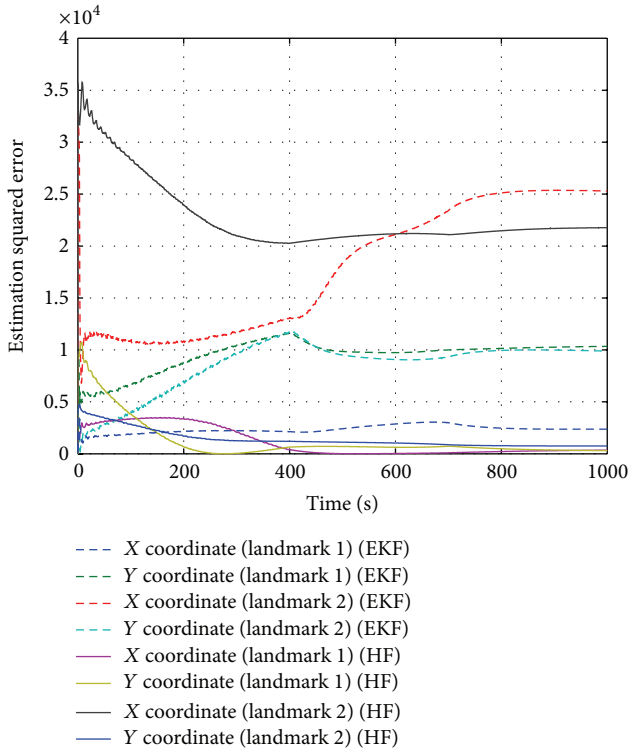


FIGURE 10: Case 2: RMSE performance between  $H_\infty$  filter and EKF.

is satisfied in each observation. However, if the proposed conditions are not fulfilled, then the estimation becomes erroneous as explained in the literature [28], where EKF performs better.

Even though it is imperative to ensure that the conditions specified under Theorems 5 and 6 are satisfied, note that initial state covariance and process noise have the possibilities to influence the estimation. Bigger process noise contributes to a bigger selection of  $\gamma$  as it may be observed from (10). Similar pattern is also observed on the initial state covariance, in which greater value of initial state covariance of heading angle may lead to unexpected result [19]. Therefore, the designer should be aware in selecting those parameters in addition to fulfilling the conditions of Theorems 3, 5, and 6.

It could be observed that the  $H_\infty$  filter estimations are much superior to the EKF even when it comes to the Gaussian noise environment with an appropriate selection of  $\gamma$  and other parameters design. Moreover, our results support the analysis discovered in [26] as the state error covariance update converges almost to zero in the estimation. In addition, it is also found that the EKF estimation becomes more inconsistent as the initial state covariance becomes bigger [19]. This is in contrast to the EKF, where even if the initial state covariance has a much bigger value, the  $H_\infty$  filter still preserves better estimation. To conclude,  $H_\infty$  filter-based SLAM is one of the competitive solutions for SLAM especially for bigger initial state covariance and non-Gaussian noise environment.

## 5. Conclusion

This study has demonstrated that the  $H_\infty$  filter may be considered as one of the best candidates to mitigate navigation issues for SLAM especially for an environment with unknown noise characteristics. It could be concluded from the two case studies that the measurement noise must be less than

$\gamma^2$  for a system with small process noise. Extra attention is required by the designers if both initial state covariance and process noise are larger, which consequently demands a bigger  $\gamma$  selection for the whole system to operate efficiently. However, to sufficiently achieve an expected performance in  $H_\infty$  filter, the designer must ensure that the above given conditions are satisfied in their system design, taking into consideration the conditions of initial state covariance, process, and measurement noises distributions.

## Conflict of Interests

The authors declare that there is no conflict of interests regarding the publication of this paper.

## Acknowledgments

The authors would like to thank the Ministry of Education (MoE), Malaysia, Research and Innovation Department of Universiti Malaysia Pahang (UMP), and Namerikawa Laboratory members for their continuous support and comments. This research is partly funded by the MoE Grant KPM-RDU130106 and internal Grant UMP-GRS130360.

## References

- [1] H. Wang, G. Fu, J. Li, Z. Yan, and X. Bian, "An adaptive UKF based SLAM method for unmanned underwater vehicle," *Mathematical Problems in Engineering*, vol. 2013, Article ID 605981, 12 pages, 2013.
- [2] M. E. West and V. L. Syrmos, "Navigation of an autonomous underwater vehicle (AUV) using robust SLAM," in *Proceedings of the IEEE International Conference on Control Applications (CCA '06)*, pp. 1801–1806, Munich, Germany, October 2006.
- [3] A. Nüchter, H. Surmann, K. Lingemann, J. Hertzberg, and S. Thrun, "6D SLAM with an application in autonomous mine mapping," in *Proceedings of the IEEE International Conference on Robotics and Automation*, pp. 1998–2003, New Orleans, La, USA, April 2004.
- [4] S. Thrun, W. Burgard, and D. Fox, *Probabilistic Robotics*, The MIT Press, Cambridge, Mass, USA, 2005.
- [5] R. Zlot and M. Bosse, "Efficient large-scale 3D mobile mapping and surface reconstruction of an underground mine," in *Proceedings of the Field and Service Robotics*, pp. 479–493, January 2014.
- [6] P. Henry, M. Krainin, E. Herbst, X. Ren, and D. Fox, "RGB-D mapping: using Kinect-style depth cameras for dense 3D modeling of indoor environments," *International Journal of Robotics Research*, vol. 31, no. 5, pp. 647–663, 2012.
- [7] C. Forster, S. Lynen, L. Kneip, and D. Scaramuzza, "Collaborative monocular SLAM with multiple micro aerial vehicles," in *Proceedings of the IEEE/RSJ International Conference on Intelligent Robots and Systems*, pp. 3962–3970, Tokyo, Japan, November 2013.
- [8] M. T. Lazaro, L. M. Paz, P. Pinies, J. A. Castellanos, and G. Grisetti, "Multi-robot SLAM using condensed measurements," in *Proceedings of the IEEE/RSJ International Conference on Intelligent Robots and Systems*, pp. 1069–1076, Tokyo, Japan, November 2013.
- [9] S. Saeedi, L. Paull, M. Trentini, and H. Li, "Neural network-based multiple robot simultaneous localization and mapping," *IEEE Transactions on Neural Networks*, vol. 22, no. 12, pp. 2376–2387, 2011.
- [10] K. Çelik and A. K. Somani, "Monocular vision SLAM for indoor aerial vehicles," *Journal of Electrical and Computer Engineering*, vol. 2013, Article ID 374165, 15 pages, 2013.
- [11] A. J. Davison, I. D. Reid, N. D. Molton, and O. Stasse, "MonoSLAM: real-time single camera SLAM," *IEEE Transactions on Pattern Analysis and Machine Intelligence*, vol. 29, no. 6, pp. 1052–1067, 2007.
- [12] A. Chatterjee and F. Matsuno, "A neuro-fuzzy assisted extended kalman filter-based approach for simultaneous localization and mapping (SLAM) problems," *IEEE Transactions on Fuzzy Systems*, vol. 15, no. 5, pp. 984–997, 2007.
- [13] C. Fu, M. A. Olivares-Mendez, R. Suarez-Fernandez, and P. Campoy, "Monocular visual-inertial SLAM-based collision avoidance strategy for fail-safe UAV using fuzzy logic controllers," *Journal of Intelligent Robotic Systems*, vol. 73, no. 1–4, pp. 513–533, 2014.
- [14] H. Ahmad and T. Namerikawa, "Intermittent measurement in robotic localization and mapping with FIM statistical bounds," *IEEJ Transactions on Electronics, Information and Systems*, vol. 131, no. 6, pp. 1223–1232, 2011.
- [15] P. Muraca, P. Pugliese, and G. Rocca, "An extended Kalman Filter for the state estimation of a mobile robot from intermittent measurements," in *Proceedings of the 16th Mediterranean Conference on Control and Automation (MED '08)*, pp. 1850–1855, Ajaccio Corsica, France, June 2008.
- [16] P. M. Lynch and J. F. Figueroa, "Position estimation with intermittent measurements," in *Proceedings of the American Control Conference*, pp. 2280–2285, Boston, Mass, USA, June 1991.
- [17] M. W. M. Gamini Dissanayake, P. Newman, S. Clark, H. F. Durrant-Whyte, and M. Csorba, "A solution to the simultaneous localization and map building (SLAM) problem," *IEEE Transactions on Robotics and Automation*, vol. 17, no. 3, pp. 229–241, 2001.
- [18] J. Nieto, T. Bailey, and E. Nebot, "Can-SLAM: combining EKF-SLAM and scan correlation," *Field and Service Robotics*, vol. 25, pp. 167–178, 2006.
- [19] S. Huang and G. Dissanayake, "Convergence and consistency analysis for extended Kalman filter based SLAM," *IEEE Transactions on Robotics*, vol. 23, no. 5, pp. 1036–1049, 2007.
- [20] J. A. Castellanos, R. Martinez-Cantin, J. D. Tardós, and J. Neira, "Robocentric map joining: improving the consistency of EKF-SLAM," *Robotics and Autonomous Systems*, vol. 55, no. 1, pp. 21–29, 2007.
- [21] L. M. Paz, J. D. Tardós, and J. Neira, "Divide and conquer: EKF SLAM in  $O(n)$ ," *IEEE Transactions on Robotics*, vol. 24, no. 5, pp. 1107–1120, 2008.
- [22] L. D'Alfonso, A. Grano, P. Muraca, and P. Pugliese, "Sensor fusion and surrounding environment mapping for a mobile robot using a mixed extended Kalman filter," in *Proceedings of the 10th IEEE International Conference on Control and Automation (ICCA '13)*, pp. 1520–1525, Hangzhou, China, June 2013.
- [23] M. Montemerlo and S. Thrun, "Simultaneous localization and mapping with unknown data association using FastSLAM," in *Proceeding of the IEEE International Conference on Robotics and Automation*, pp. 1985–1991, Karlsruhe, Germany, September 2003.

- [24] F. Pei, M. Wu, and S. Zhang, "Distributed SLAM using improved particle filter for mobile robot localization," *The Scientific World Journal*, vol. 2014, Article ID 239531, 10 pages, 2014.
- [25] D. Simon, "From here to infinity," in *Embedded Systems Programming*, pp. 72–79, 2001.
- [26] H. Ahmad and T. Namerikawa, " $H_\infty$  filter convergence and its application to SLAM," in *Proceedings of the ICROS-SICE International Joint Conference*, pp. 2875–2880, Fukuoka, Japan, August 2009.
- [27] H. Ahmad and T. Namerikawa, "Feasibility study of partial observability in  $H_\infty$  filtering for robot localization and mapping problem," in *Proceedings of the American Control Conference (ACC '10)*, pp. 3980–3985, Baltimore, Md, USA, July 2010.
- [28] H. Ahmad and T. Namerikawa, "Robot localization and mapping problem with unknown noise characteristics," in *Proceedings of the IEEE International Conference on Control Applications (CCA '10)*, pp. 1275–1280, Yokohama, Japan, September 2010.
- [29] H. Ahmad and T. Namerikawa, "Robotic mapping and localization considering unknown noise statistics," *Journal of System Design and Dynamics*, vol. 5, no. 1, pp. 70–82, 2011.
- [30] P. Bolzern, P. Colaneri, and G. De Nicolao, " $H_\infty$  differential Riccati equations: convergence properties and finite escape phenomena," *IEEE Transactions on Automatic Control*, vol. 42, no. 1, pp. 113–118, 1997.
- [31] P. Bolzern and M. Maroni, "New conditions for the convergence of  $H_\infty$  filters and predictors," *IEEE Transactions on Automatic Control*, vol. 44, no. 8, pp. 1564–1568, 1999.
- [32] J. Andrade-Cetto and A. Sanfeliu, *Environment Learning for Indoor Mobile Robots*, Springer, 2006.
- [33] T. Vidal-Calleja, J. Andrade-Cetto, and A. Sanfeliu, "Conditions for suboptimal filter stability in SLAM," in *Proceedings of the IEEE/RSJ International Conference on Intelligent Robots and Systems (IROS '04)*, pp. 27–32, Sendai, Japan, October 2004.



# Hindawi

Submit your manuscripts at  
<http://www.hindawi.com>

